

NGR-31-003-020

Critical Temperatures and Critical Fields of
Multiple Superconducting and Normal Conducting Films.*†

R. J. Duffy^{††} and Hans Meissner

Department of Physics, Stevens Institute of Technology

Hoboken, New Jersey

(Received

)

The critical temperatures and critical magnetic fields have been determined for a series of superposed normal and superconducting films. Both Cu-Sn and Au-Sn samples were investigated. The samples were prepared by vacuum deposition methods or by electroplating. Thicknesses of the Sn films ranged from 160 Å to 2700 Å. The dependence of the critical temperature T_c of the multiple film on normal metal thickness is compared with recent theories. Experimental evidence is given that the observed effects are true proximity effects, caused by the free exchange of electrons between the two metals and that metallic diffusion alone is not responsible for the observed phenomena. The critical magnetic fields of both single and multiple films are compared with the microscopic theories. It is shown that at fields near the critical fields with the multiple film still superconducting the gap function $\Delta(r)$ and the magnetization are negligibly small on the normal side of the film.

* Based on a thesis submitted to the Department of Physics of Stevens Institute of Technology in partial fulfillment of the requirements for the Ph. D. degree.

† Supported in part by the National Aeronautic and Space Agency.

†† Present address: National Bureau of Standards, Institute for Materials Research, Boulder, Colorado.

FACILITY FORM 602	N 66 86804	
	(ACCESSION NUMBER)	(THRU)
	30	None
	(PAGES)	(CODE)
	CK-68750	
	(NASA CR OR TMX OR AD NUMBER)	(CATEGORY)

I. INTRODUCTION

If a thin specimen of a superconducting metal is in intimate contact with a normal conducting metal (or another superconductor which is still in the normal state at the temperature in question), the value of the critical temperature T_c is lower than the value for the superconductor alone. Many recent experiments¹⁻⁸ have investigated this phenomenon and several theoretical explanations have been proposed.^{6,7,9-12} Werthamer^{7,11} and deGennes¹² have shown that such a proximity effect should exist due to a change in the gap-function $\Delta(\underline{r})$. The value of $\Delta(\underline{r})$ is altered in the superconductor due to the presence of the normal metal and takes on a non-zero value in the normal side. The lowest eigenvalue of their equation for $\Delta(\underline{r})$ gives the value of T_c for each sample. In general $\Delta(\underline{r})$ is a function of the magnetic field and goes to zero at the critical magnetic field H_c . Since $\Delta(\underline{r})$ is altered by the presence of a normal metal, H_c also should vary as a function of the thickness of the normal metal.

In this paper we present our results of the determination of T_c and H_c^{\wedge} ^(parallel to the film) for thin multiple film samples. Our samples were made by vacuum deposition of the metals on glass substrates. Resistance measurements were used to determine H_c as a function of temperature. To obtain meaningful data in this way, it was necessary to mechanically trim the sample edges, assuring a constant film thickness. Thus each sample was at room temperature for a short time, causing some unavoidable diffusion between the two metals.

In section II we present the experimental procedures used for fabricating the samples and for determining the resistance, T_c , and H_c of each sample. Section III discusses the resistances of each set of samples showing the effects of diffusion. In section IV we present the data for T_c and show the effects of diffusion and of

the proximity of the normal metal on the value of T_c . Section V then treats H_c both for single and composite films. The results are analyzed in terms of the theories of deGennes¹⁴ and deGennes and Tinkham¹³ which provide a rigorous treatment of the critical field of alloyed thin films, and which are known to agree quite well with experiment.¹⁵

II. EXPERIMENTAL PROCEDURES

A. Samples

The samples were prepared in a high vacuum evaporator. Tin was chosen as the superconductor and both gold and copper were used as the normal metal. The thickness of the Sn films, d_s , was in the range of 160 Å to 2700 Å. The thickness of the normal metal, d_n , ranged from 0.1 d_s to 1.0 d_s . Because of the high values of H_c for the thinnest samples, H_c was only determined for the larger values of d_s . For all films investigated the magnetic transition was of second order, i.e. $\Delta(r)$ went to zero continuously as H approaches H_c . This is the usual case treated by theories^{13,14,16}

The samples were made in the shape of an "H" by placing a metal mask in front of the substrates. This gave a film of uniform thickness except for the penumbra around the edges, which was removed by trimming each side with a scalpel. To control the resulting diffusion between the two metals, a special evaporator was designed to produce an entire set of multiple samples at the same time. The value of d_s was held constant and d_n was varied for each sample of the set. The thermal history of all samples in a set was kept identical.

It was possible to produce a set of eight composite films, one Sn film as well as a separate series of small single films, the latter to be used for the optical determination of the thicknesses.¹⁷ With a slight modification, four composite films,

four single normal films and one Sn film could be made. The metals could be evaporated in either order, but in general it was better to deposit the normal metal first, where different thicknesses were achieved by moving a shutter, and then to deposit a constant layer of Sn. This insured that each sample was exposed to the radiation from the molten Sn for the same length of time.

The metals were evaporated from molybdenum heaters each of which was shielded to permit outgassing of the metals in the molten state. The substrates were cut from commercial microscope slides, cleaned with methanol in an ultrasonic cleaner and clamped against a brass block in the evaporator. Springs made of phosphor bronze maintained thermal contact between the glass and the brass block which could either be cooled with liquid nitrogen or heated with a Nichrome heater. The temperature of the block was monitored with a thermocouple. A liquid helium cold trap was positioned between the sample holder and the pumping line. It reduced the partial pressures of O_2 , H_2 , and CO_2 which are known to influence the critical fields of thin films.¹⁸ The total pressure during evaporation was less than 4×10^{-7} torr..

During deposition the substrate holder was cooled with a constant flow of liquid nitrogen. The resulting crystal size was about 800 \AA for $d_s = 1000 \text{ \AA}$. For the case of the Cu-Sn samples, the films would crack if both metals were deposited consecutively onto the cold substrates. It was necessary to anneal the Cu films at 200°C for a few minutes before recooling the substrates for the deposition of Sn. The total time for the heating and recooling was 45 minutes. For the Au-Sn samples this procedure was not necessary and the two films were deposited consecutively.

After the evaporation was completed, helium gas was admitted into the vacuum chamber to warm the samples to room temperature. They were then removed and stored in liquid nitrogen. They were later brought back to room temperature, two at a time,

trimmed and mounted in the experimental cryostat. The total time at room temperature was always between 90 and 120 minutes.

For purposes of comparison, two additional methods were used for making samples. One set was made by vacuum deposition of eight Sn films and then gold was electroplated onto each. A gold cyanide solution (Baker & Co. No 319) was used with a plating current density of 5 ma/cm^2 . A second set was made by first depositing four identical composite films in the evaporator. Then various amounts of gold were removed electrolytically in a potassium cyanide solution. The current density was again 5 ma/cm^2 . We shall refer to these as "polished samples."

In all, 12 sets of samples were prepared. Details about their resistances, critical temperatures and the measured values of $H_c(T)$ can be found in the thesis.¹⁹

B. Measurements

The samples were mounted ^{parallel to the applied magnetic field,} in a niobium field coil which had overwound ends and was capable of providing a field of 4000 Oe with a uniformity of better than 0.1% over the volume occupied by the samples. Since the critical fields, H_c , of our samples were always quite large the earth's field was not compensated.

The field coil was mounted in the inner vessel of a double Dewar cryostat.¹⁹ A high capacity pumping system lowered the temperature of the inner vessel to 0.8°K , while the outer helium bath could be pumped down to 1.2°K .

The temperature of the inner bath was determined by vapor pressure measurements,²⁰ or, at the lowest temperatures, by a calibrated carbon resistance thermometer.

Both T_c and $H_c(T)$ were determined by observing the resistance transition from

the normal to the superconducting state and were defined as the point of 50% of the normal resistance. The critical field transitions were plotted with an x-y recorder and were reversible as expected for second order transitions. The value of T_c was also checked by extrapolating the $H_c(T)$ data to zero field. H_c was determined to within 2%, while T_c was determined to ± 0.01 °K.

The resistance of the samples was measured with a four terminal network and precision potentiometer. A Leeds and Northrup DC microvolt amplifier was used for finding the null position.

The thickness of each film was determined by using fringe shifts of equal chromatic order.¹⁷ The single films which had been made during the production of the samples were removed from the evaporator and within a few minutes were covered with a thick layer of aluminum in another evaporator. The subsequent measurements determined each thickness to an accuracy of ± 30 Å. For films thinner than 150 Å a calibration of thickness vs. time of evaporation was used. We estimate that these values are accurate to 20%.

Figures 1 and 2 show some typical data for our samples. Figure 1 shows the reduced critical temperature $\mathcal{T} = T_c/T_{cs}$ as a function of d_n for Cu-Sn samples. T_c is the critical temperature for the composite sample and T_{cs} is its value for the single Sn film. The behavior in general is what is found by other investigators. The slight differences will be discussed later. Figure 2 shows $H_c(T)$ vs. T^2 for a set of Au-Sn samples. It shows the general behavior that was found for these samples namely, T_c decreases and $H_c(0)$ increases as d_n is increased. The temperature dependence of $H_c(T)$ is that expected for thin films with limited electronic mean free paths.

III. RESISTIVITY

We found that the resistive properties of our multiple films were quite different from those of single films. The electronic mean free path ℓ in the composite samples was greatly reduced below the value in a bare Sn film where $\ell \sim d_s$.

Figure 3 shows the resistance at 4.2 °K in Ω/sq of a set of samples as a function of the total thickness $d = d_s + d_n$ of the two films. Thus the Sn film with $d_n = 0$ is plotted at $d = 775 \text{ \AA}$. The resistance increases very rapidly as d_n increases, showing quite clearly that diffusion has taken place between the two metals. The resistance then begins to decrease as d_n is further increased.

It is clear that the values of the resistivities ρ for single films are useless for an analysis of our data. We have therefore used the following method to deduce a reasonable value of ρ and ℓ for our samples. On the same plot we have drawn a family of curves which give the resistance in Ω/sq vs. film thickness for a material characterized by a bulk mean free path ℓ_0 and the constant ρ_0 , $\rho_0 \ell_0 = 1.12 \times 10^{-11} \Omega \text{cm}^2$. The curves were calculated using Sondheimer's relation²¹ for diffuse scattering. The value of the constant^{22,23} $\rho_0 \ell_0$ is an average value that can be used for Sn and Au with an error of about 10%.

The point for the single Sn film has a value of ℓ_0 which is approximately equal to d_s . As gold is added the resistance increases and the effective value of ℓ_0 decreases until it remains constant at approximately 60 \AA . It seems reasonable to assume that for these last samples 60 \AA should give a good estimate for ℓ_0 in both films. For the samples with small d_n the value of ℓ_0 should be a good estimate in the Sn but not necessarily in the Au. For thicker tin films, d_s 1000 \AA , the final value of ℓ_0 is much larger, about $\ell_0 = 200 \text{ \AA}$.

If $\ell_c \ll d$ then the actual mean free path ℓ is equal to ℓ_0 . For $\ell_0 \sim d$ we can use the relation

$$\ell = \rho_0 \ell_0 / \rho \quad (1)$$

This expresses the fact that the product $\rho \ell$ is approximately a constant for a given metal. The value for ρ is taken as $\rho = R_4 (d_s + d_n)$ (Note that R_4 is in Ω/sq).

IV. CRITICAL TEMPERATURES

The theories of deGennes¹² and Werthamer^{7,11} give the following two relations for T_c of a composite sample,

$$\ln(T_{cs}/T_c) = \chi(\xi_s^2 k_s^2) ; \quad \ln(T_c/T_{cn}) = -\chi(-\xi_n^2 k_n^2) \quad (2)$$

and

$$N_s \xi_s^2 k_s \tan(k_s d_s) = N_n \xi_n^2 k_n \tanh(k_n d_n) \quad (3)$$

the latter follows from the boundary conditions at the interface of the two metals.

Here T_{cs} and T_{cn} are the transition temperatures of the individual films and N is the density of electron states at the Fermi surface of each metal. The function $\chi(z)$ is given by

$$\chi(z) \equiv \psi\left(\frac{1}{2} + \frac{1}{2}z\right) - \psi\left(\frac{1}{2}\right) \quad (4)$$

where ψ is the digamma function, and ξ_i is given by

$$\xi_i = (\hbar v_F \ell / 6 \pi k_B T_c)_i^{1/2} \quad (5)$$

where v_F is the Fermi velocity, ℓ is the electronic mean free path in each metal and k_B is the Boltzmann constant, the subscript i refers to either n (normal) or s (superconducting) metal.

Assuming that $T_{cn} \sim 0$ and using the expansion for $\chi(z)$ in reference 11 we find

that (2) becomes

$$k_s = (2/\pi \xi_{ss}) (1-\tau)^{\frac{1}{2}} \quad ; \quad k_n = (1/\xi_{ns}) \tau^{\frac{1}{2}} \quad (6)$$

where $\tau = T_c/T_{cs}$.

Here ξ_i is normalized to $\tau = 1$ and the relation $\xi_i = \xi_{i,1} \tau^{-\frac{1}{2}}$ has been used. The quantities k_i describe the variation of $\Delta(r)$ in each metal.

Combining equations (6) and (3) then gives

$$\left(\frac{1-\tau}{\tau}\right)^{\frac{1}{2}} = \frac{\pi}{2} \left(\frac{N_n \xi_{ns}}{N_s \xi_{ss}} \right) \frac{\tanh(k_n d_n)}{\tan(k_s d_s)} \quad (7)$$

This is not an explicit equation for τ since k_n and k_s each are functions of τ . In addition both k_i and ξ_i are functions of ℓ and thus change from sample to sample. To avoid these difficulties, we focus our attention near $\tau = 1$ where k_s and d_n are small. Expanding the right hand side of (7) to first order gives

$$\frac{1-\tau}{\tau} = \frac{\pi^2}{4} \frac{N_n d_n}{N_s d_s} \quad (8)$$

From Eq. (8) we obtain for the initial slope of the curves of Fig. 1 and 5:

$$\left(\Delta d_n / \Delta \tau\right)_{\tau=1} = - \frac{4}{\pi^2} \frac{N_s}{N_n} d_s \quad (9)$$

The initial slope is determined by the ratio of the density of states in the two metals and the thickness of the superconductor.

In Figure 4 we have plotted $-(\Delta d_n / \Delta \tau)_{\tau=1}$ vs. d_s for both Cu-Sn and Au-Sn samples. The two straight lines represent the slope $(4/\pi^2) (N_s/N_n)$ for both combinations, where we have used the relation $(N_s/N_n) = (\gamma_s/\gamma_n)$, γ being the coefficient of the electronic specific heat;^{24,25} $\gamma_{Sn} = 1.09 \times 10^3$ erg/deg² cm³, $\gamma_{Au} = 0.730 \times 10^3$ erg/deg² cm³, and $\gamma_{Cu} = 0.688$ erg/deg² cm³. The agreement gets poorer as d_s increases which is in part due to the expansion of $\tan(k_s d_s)$.

Next we wish to discuss the effects of a change in ℓ . If we look again at figure 1

we see two types of behavior. The curves for large d_s show that in the limit of large d_n τ assumes a constant value. The curves for small d_s , however, do not show any limiting behavior. DeGennes has pointed out that both behaviors should be expected depending on whether the film thickness is larger or smaller than ξ . For $d_{n,s} > \xi_{n,s}$ he shows that τ drops rapidly and goes to zero for some finite value of d_n . For $d_{n,s} < \xi_{n,s}$ the value of τ reaches a limiting value as $d_n \rightarrow \infty$.

With this in mind we have investigated the relative magnitudes of d_s and ξ_s for our films. By rewriting equation (5) using the relation

$$v_F l = (\pi k_B / e)^2 / 8 \gamma \quad (10)$$

we find

$$\xi_i^2 = (\pi k_B / 6 e^2 T_c) / (8 \gamma)_i \quad (11)$$

For our Sn films we have used a value for ρ as discussed in Sec. III and γ_{sn} as for Fig. 4. We have assumed that γ does not change appreciably due to impurities. With these assumptions, d_s was found to be smaller than ξ_s for $d_s = 160 \text{ \AA}$. Thus we do not expect to see a limiting value for τ in agreement with Fig. 1.

The curve for $d_s = 510 \text{ \AA}$ shows an interesting behavior. The level portion is followed by a slight drop. The resistance data indicated that ℓ for the last two points was larger than for the preceeding two points. This indicated that the behavior of τ changed from one form to the other. We found that $\xi_s \sim 400 \text{ \AA}$ for the level position and that it rose to $\xi_s \sim 460 \text{ \AA}$ for the final two points. Although both values are smaller than $d_s = 510 \text{ \AA}$ it still seems most likely that the drop in τ is due to the increase of ξ_s .

Figure 5 shows τ vs. d_n for some Sn-Au samples. One set, which is of particular interest, consists of the "polished" samples discussed in Sec. II. If

the majority of the effects seen for composite films were due to diffusion or alloy formation at the metal interface, then removing gold from the outer face would have little or no effect on the value of $\tilde{\tau}$. If a proximity effect exists, then the total amount of gold is important. Data points for these "polished" samples (which all had the same thermal histories as our other samples) are shown by the squares.

The value of $\tilde{\tau}$ increases as Au is removed and the curve compares very well with the data for our other samples.

This proves unambiguously that we are observing a proximity effect as predicted by theory. However, $\tilde{\tau}$ is not a simple function of d_n since ξ changes from sample to sample due to the changes in ℓ . A more detailed analysis of the critical temperatures therefore ^{does not seem to be} worthwhile.

V. CRITICAL MAGNETIC FIELDS

A. Single Sn Films

In addition to multiple samples, the critical fields H_c of single Sn films were investigated. Since all our samples are "dirty" superconductors we will use the recent theories of deGennes¹⁴ and deGennes and Tinkham¹³ to discuss our results.

For a "dirty" superconductor in a magnetic field, deGennes has shown that at the nucleation field $H_c(T)$, $\Delta(\underline{r})$ is the smallest eigenfunction of the equation

$$[-i\nabla - (2\pi/\phi_0)\underline{A}]^2 \Delta(\underline{r}) = (\xi_0/D) \Delta(\underline{r}) \quad (12)$$

and that the eigenvalue \mathcal{E}_0 has a temperature dependence given by

$$\ln(1/t) = \chi(\mathcal{E}_0 \hbar / 2\pi k_B T_c t) \quad (13)$$

where $\chi(z)$ is the function we discussed in Section IV. In these equations $D = (1/3)v_F \ell$, ϕ_0 is the flux quantum $hc/2e$ and $t = T/T_c$, where T_c is the critical temperature of the sample and T is some lower temperature.

Near $t = 1$, $\ln(1/t) \sim 0$ and we can again expand $\chi(z)$ as we did before. This gives

$$\mathcal{E}_0 = (8k_B T_c / \pi \hbar)(1-t) \quad (14)$$

Then $H_c(t)$ can be found by solving equation (12) for \mathcal{E}_0 which is a function of H . Equation 14 then gives the temperature dependence near $t = 1$.²⁶

It can be shown that \mathcal{E}_0/D is equal to $1/\xi(t)^2$, where $\xi(t)$ is the coherence distance as a function of temperature. If $\xi(t) \ll d$, the film thickness, surface superconductivity exists up to a field H_{c3} . In this case $\mathcal{E}_0 = 0.59 (2\pi D H / \phi_0)$ giving

$$H_{c3} = (2.06 k_B T_c \phi_0 / \hbar v_F \ell)(1-t) \quad (15)$$

and near $t = 1$, the temperature dependence is linear. For $d < \xi(t)$, deGennes and Tinkham consider two cases. For Case I where $\ell < d < \xi(t)$, they find $\mathcal{E}_0 = (2\pi)^2 D H^2 d^2 / 12 \phi_0^2$ giving

$$H_c(t) = (6\sqrt{2} / \pi^{\frac{3}{2}}) (k_B T_c / \hbar v_F \ell)^{\frac{1}{2}} (\phi_0 / d) (1-t)^{\frac{1}{2}} \quad (16)$$

For Case II, $d < \ell < \xi(t)$ and $\mathcal{E}_0 = \pi^2 v_F H^2 d^3 / 16 \phi_0^2$ giving

$$H_c(t) = (8\sqrt{2} / \pi^{\frac{3}{2}}) (k_B T_c / \hbar v_F)^{\frac{1}{2}} (\phi_0 / d^{\frac{3}{2}}) (1-t)^{\frac{1}{2}} \quad (17)$$

In both cases $H_c(t) \propto (1-t)^{1/2}$.

To decide which expression of $H_c(t)$ is appropriate for our data, we plotted $H_c(t)$ both as a function of $(1-t)$ and $(1-t)^{\frac{1}{2}}$. Figure 6 shows the plot of $H_c(t)$ vs.

$(1-t)^{\frac{1}{2}}$. The data near $t = 1$ give a series of straight lines for ^{the} various samples. A corresponding plot of $H_c(t)$ vs. $(1-t)$ clearly showed that H_{c3} is not observed for our films. This result is not surprising since in the region of $t = 1$, $\xi(t) \propto (1-t)^{-\frac{1}{2}}$. By staying close enough to $t = 1$ the condition $d < \xi(t)$ can be satisfied. We observed for some very dirty samples, that a linear temperature dependence existed for $t < 0.95$.

All our H_c data for both single and multiple films were plotted vs. $(1-t)^{\frac{1}{2}}$ to insure that they were all in the proper limit and to check the observed values of T_c by extrapolating the curves to $H = 0$. Since all the curves are linear at $t = 0.96$, we chose this value of H_c to be compared with equations (16) or (17) i.e. we defined $H_c^* = H_c(0.96)$.

To analyze our H_c data for single Sn films it is necessary to know the ratio of ℓ/d . For $\ell/d < 1$, H_c^* should be plotted as a function of $d^{-1} \ell^{-\frac{1}{2}}$. For $\ell/d > 1$ the appropriate plot would be as a function of $d^{-3/2}$. The resistances indicate that for all the single films $\ell \sim d$ making it necessary to look at both functional dependences. With this in mind we rewrite equations (16) and (17) as

$$H_c(t) = \alpha_1 \frac{\phi_0}{d(\xi_0 d)^{\frac{1}{2}}} \left(\frac{d}{\ell}\right)^{\frac{1}{2}} (1-t)^{\frac{1}{2}} = \beta_1 \frac{\phi_0 e}{\pi} \left(\frac{\gamma T_c}{\hbar k_B}\right)^{\frac{1}{2}} \frac{\sqrt{\ell}}{d} (1-t)^{\frac{1}{2}} \quad (18)$$

for $\ell/d < 1$ and

$$H_c(t) = \alpha_2 \frac{\phi_0}{d(\xi_0 d)^{\frac{1}{2}}} (1-t)^{\frac{1}{2}} = \beta_2 \frac{\phi_0 e}{\pi} \left(\frac{\gamma T_c}{\hbar k_B}\right)^{\frac{1}{2}} \frac{\sqrt{\ell}}{d} \left(\frac{\ell}{d}\right)^{\frac{1}{2}} (1-t)^{\frac{1}{2}} \quad (19)$$

for $\ell/d > 1$, where we use the relation $\xi_0 = 0.18 (\hbar v_F / k_B T_c)$ and Eq. (10). The numerical constants are grouped into the factors $\alpha_1 = 0.65$, $\alpha_2 = 0.86$, $\beta_1 = 1.53$, $\beta_2 = 2.03$, with $\beta/\alpha = 2.36$ for both cases.

If H_c^* is plotted as a function of $\sqrt{\ell}/d$ then all those samples with $\ell/d < 1$ should fall on a universal curve, while those with $\ell/d > 1$ should scatter somewhat, depending on their individual ℓ/d ratios. Fig. 7a shows that indeed 4 samples fall

on the same curve (the lower one) and an inspection of their resistances (see Eq. 1) shows that for these $\ell/d < 1$. Plotting H_c^* as a function of $d^{-3/2}$ should reverse the situation, all those samples with $d/\ell > 1$ should fall on a universal curve while those with $d/\ell < 1$ should scatter somewhat, depending on their individual ℓ/d ratios. Fig. 7b, however, shows that all sample points fall on the same line. This indicates that accidentally the ℓ/d ratios of the ^{two} groups of samples are fairly uniform and of such a value to give a single curve on this plot, one being $\ell/d = 0.72$, the other $\ell/d = 1.10$. Using the value of χ_{sn}^p as given above and of $T_c = 3.80^\circ\text{K}$ we find from the slopes of the curves of Fig. 7 $\alpha_1 = 0.52$ and $\alpha_2 = 0.61$ in reasonable agreement with the values of the constants listed above.

The curves of Fig. 7 can then be used to find the values of ℓ/d from Eq. (19) or (20) respectively and, with the thickness of the film, the value of the electronic mean free path ℓ .

In table I the values of ℓ obtained in this fashion are compared with those obtained from the resistivities, using Eq. 1.

Table I: Electronic mean free paths
for single tin films

Sample	1	2	3	4	5	6	7
ℓ_a (Å)	1250	850	830	1100	564	187	760
ℓ_b (Å)	1320	850	828	1100	558	368	715
d_s (Å)	1200	1180	1150	1000	775	510	990

$$\ell_a = \rho_o \ell_o / \rho_4 \text{ with } \rho_o \ell_o = 1.05 \times 10^{-11} \Omega \text{cm}^2$$

ℓ_b = value calculated from $H_c(T)$ data using equations (18) and (19) respectively.

B. Multiple Films

For the case of multiple films the solutions (16) and (17) should not hold exactly, since the restriction on $\Delta(r)$ to derive equation (12) (that it be constant) is no longer valid. In addition, the solution for ξ_0 involves boundary conditions for $\Delta(r)$ which are different for the two cases.

In our experiment, since we measure the sample's resistance, we do not observe any change until the magnetic field has caused the energy gap to fall to zero in both metal films. Since the energy gap is much smaller in the normal side, it is most likely that it can be zero there while a non-zero value remains in the superconductor.

Under these conditions the assumption that $\Delta(r)$ is a constant in the superconductor and that $\Delta(r) = 0$ in the normal metal may be a good one. For the case of a constant $\Delta(r)$, the problem of different boundary conditions is of no importance. And in particular the boundary conditions play no role in the solution given by equation (16). For all our composite samples $\ell/d < 1$, therefore we will proceed to present our results using equation (16) or more conveniently equation (18). Since the value of T_c changes for each composite sample we move $T_c^{1/2}$ to the left side of Eq. (18) and we plot $H_c^*/T_c^{1/2}$ as a function of $g^{1/2}/d_s$. The thickness d_s and not $d = d_s + d_n$ is used because of our assumption that $\Delta(r) = 0$ in the normal side. As before ϕ is given by $R_4(d_s + d_n)$.

In Figure 8 we show the data for two sets of Au-Sn films. (One set is plated and the other is evaporated.) For both, d_s is about 1200 Å. The curve with the larger slope has approximately the slope corresponding to $\beta_1 = 1.23$ for pure Sn with $\ell/d < 1$ in Fig. 7a. The open points are the single Sn films and have been.

corrected for their value of ℓ . They both had $\ell/d > 1$ and thus were corrected to fit the curve for $\ell/d < 1$. The majority of the points are better fitted by a curve with $\beta_1 = 0.95$, again assuming that β does not change appreciably from its value for Sn.

Considering the approximations that have been made, as well as the fact that both T_c and β exhibit large changes, one is encouraged to think that the critical fields of multiple samples can be handled by an equation such as (18). The reason for a difference in slope is not clear although it may be connected with the fact that for the samples on the lower curve $\ell \ll d$ while $\ell \sim d$ for the others.

VI. CONCLUSIONS

The measurements on the "polished" samples prove unambiguously that a proximity effect exists and that the lowering of the critical temperatures of multiple films is not primarily due to metallic diffusion.

Diffusion is certainly present in the experiments. It influences T_c and $H_c(T)$ in as much as it changes the electronic mean free path

The critical fields of multiple films agree fairly well with the following model: Near H_c the gap function $\Delta(r)$ as well as the magnetization are negligible small in the normal side of the film.

The multiple film then behaves like a single film, of thickness d_s , of the superconducting part alone with the value of the electronic specific heat approximately that of the pure metal, the critical temperature T_c of the multiple film, and an electronic mean free path ℓ of the multiple film.

The fact that d_s and not $d_n + d_s$ is important is in agreement with measurements of the microwave absorption in gold films plated onto bulk tin.^{27,28}

VII. ACKNOWLEDGMENTS

This research was in part supported by the National Aeronautic and Space Administration. The helium gas was supplied by the Office of Naval Research. Many of the larger pieces of equipment were bought with funds from the Charles and Rosanna Batchelor Memorial Foundation. The authors would like to thank J. A. Mydosh and J. Zorskie for their assistance and G. Wirth for the machining of the evaporator and the operation of the helium liquefier. One of us (R. D.) wishes to acknowledge some very helpful discussions with Dr. B. B. Goodman.

Some of the analysis was carried out while one of us (R. D.) held an N. S. F. postdoctoral fellowship at CNRS Grenoble. The financial support of the National Science Foundation and the hospitality of Prof. L. Weil during this time are gratefully acknowledged.

Figure Captions

- Fig. 1. Reduced critical temperature $\tilde{\tau} = T_c/T_{cs}$ as a function of normal film thickness d_n with superconducting film thickness d_s as a parameter. Cu-Sn films, vacuum deposited.
- Fig. 2. Critical fields of a set of gold-tin films as a function of T^2 .
- Fig. 3. Resistance at 4 °K (in Ω/sq) as a function of total film thickness $d = d_s + d_n$ for a set of vacuum deposited Au-Sn films. For comparison a family of curves are drawn for a material with $\xi_0 \ell_0 = 1.12 \times 10^{-11} \Omega \text{cm}^2$ with bulk electronic mean free path ℓ_0 as a parameter.
- Fig. 4. $\lim_{\tilde{\tau} \rightarrow 1} (-\Delta d_n / \Delta \tilde{\tau})$ as a function of d_s .
- Cu-Sn films

△ Au-Sn films
- Fig. 5. Reduced critical temperature $\tilde{\tau} = T_c/T_{cs}$ as a function of d_n for Au-Sn samples.
- vacuum deposited Au-Sn samples

■ Sn-Au samples where gold has been removed by electrolytic polishing.
- Fig. 6. Critical fields $H_c(T)$ plotted as a function of $(1-t)^{1/2}$ for the same set of Au-Sn samples shown in Fig. 2. The numbers on the curves refer to the normal metal thickness d_n .
- Fig. 7. Critical fields $H_c^* = H_c(t = 0.96)$ for single Sn films.
- a.) as a function of $\sqrt{\xi}/d$

b.) as a function of $d^{-3/2}$

Fig. 8. Critical fields $H_c^*/H_c = H_c (t = 0.96)/t_c^{1/2}$ for two sets of multiple films as a function of $\sqrt{\xi}/d_s$.

○	$d_s = 1200 \text{ \AA}$	$d_n = 0$	}	vacuum deposited
●	$d_s = 1200 \text{ \AA}$	$d_n = 55 - 540 \text{ \AA}$		
△	$d_s = 1000 \text{ \AA}$	$d_n = 0$	}	Sn vacuum deposited Au plated.
▲	$d_s = 1000 \text{ \AA}$	$d_n = 100 - 735 \text{ \AA}$		

BIBLIOGRAPHY

1. H. Meissner Phys. Rev. 117 672 (1960), IBM Journ. Res. Develop. 6 71 (1962).
2. H. Meissner Proc. 8th Int. Conf. Low Temp. Phys., Butterworths (Washington 1964), p. 365.
3. P. H. Smith, S. Shapiro, T. L. Miles and J. Nicol, Phys. Rev. Letters 6 686 (1961).
4. W. A. Simmons and D. H. Douglass Jr. Phys. Rev. Letters 9 153 (1962).
5. P. Hilsch, Z. Physik 167 511 (1962).
6. P. Hilsch and R. Hilsch, Z. Physik 180 10 (1964).
7. J. J. Hauser, H. C. Theurer and N. R. Werthamer, Phys. Rev. 136 A637 (1964).
8. J. J. Hauser and H. C. Theurer Phys. Letters 14 270 (1965).
9. L. N. Cooper Phys. Rev. Letters 6 89 (1962).
10. D. H. Douglass Jr. Phys. Rev. Letters 9 155 (1962).
11. N. R. Werthamer Phys. Rev. 132 2440 (1963).
12. P. G. DeGennes, Rev. Mod. Phys. 36 225 (1964).
13. P. G. deGennes and M. Tinkham, Physics 1 107 (1964).
14. P. G. deGennes Phys. Kondens. Materie 3 79 (1964).
15. J. P. Burger et. al. Phys. Rev. 137 A853 (1964).

16. G. Rickayzen Phys. Rev. 138 A73 (1965).
17. S. Tolansky, Multiple Beam Interferometry of Surfaces and Films, Clarendon Press, (Oxford, 1954).
18. H. L. Caswell, J. Appl. Phys. 32 105 (1961).
19. R. Duffy, Thesis, Stevens 1964 (unpublished), Microfilm copies available from Microfilms Inc., 313 First Street, Ann Arbor, Michigan.
20. F. G. Brickwedde, H. Van Dijk, M. Durieux, J. R. Clement, and J. K. Logan, J. Res. Natl. Bur. Std. (U. S.) A64, 1 (1960).
21. E. H. Sondheimer, Adv. Phys. 1 1, (1952).
22. D. K. C. MacDonald, Encyclopedia of Physics, S. Flügge, Ed., Vol. 14, p. 183 (Springer, Berlin 1956).
23. R. G. Chambers, Proc. Roy. Soc. London. A215 481 (1952).
24. H. R. O'Neal and N. E. Phillips, Phys. Rev. 137 A 748 (1965).
25. W. S. Corak, M. P. Garfunkel, C. B. Satterthwaite, and Aaron Wexler Phys. Rev. 98, 1699 (1955).
26. The Solution of Eq. (13) at $t = 0$ is $\epsilon_0 = 1.76K_B T_c / \hbar$, see ref. 13.
27. Hans Meissner and R. V. Fanelli, Revs. Mod. Phys. 36 194 (1964).
28. R. V. Fanelli and Hans Meissner, Phys. Rev. (1966).

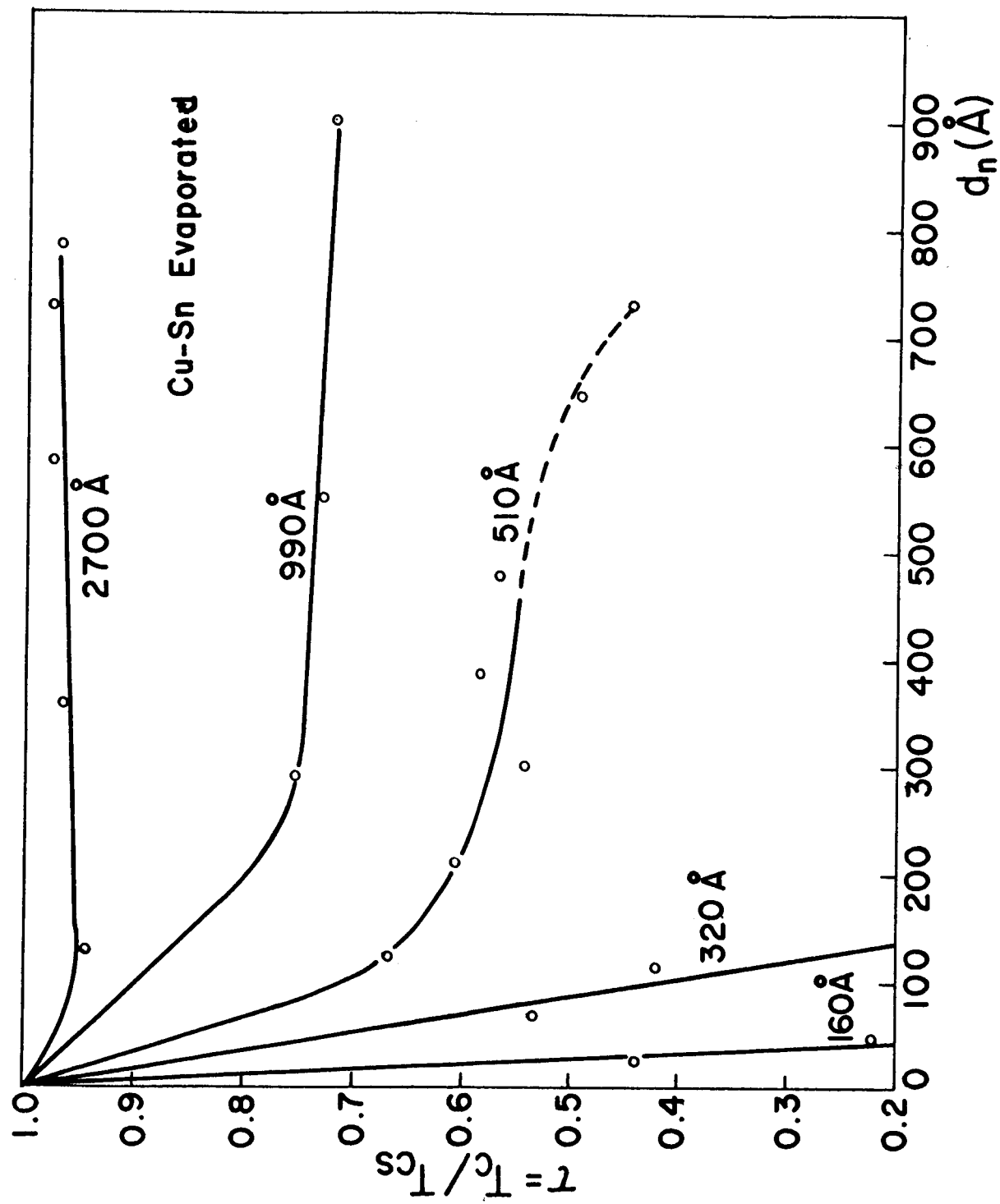


Fig 1

8-55989

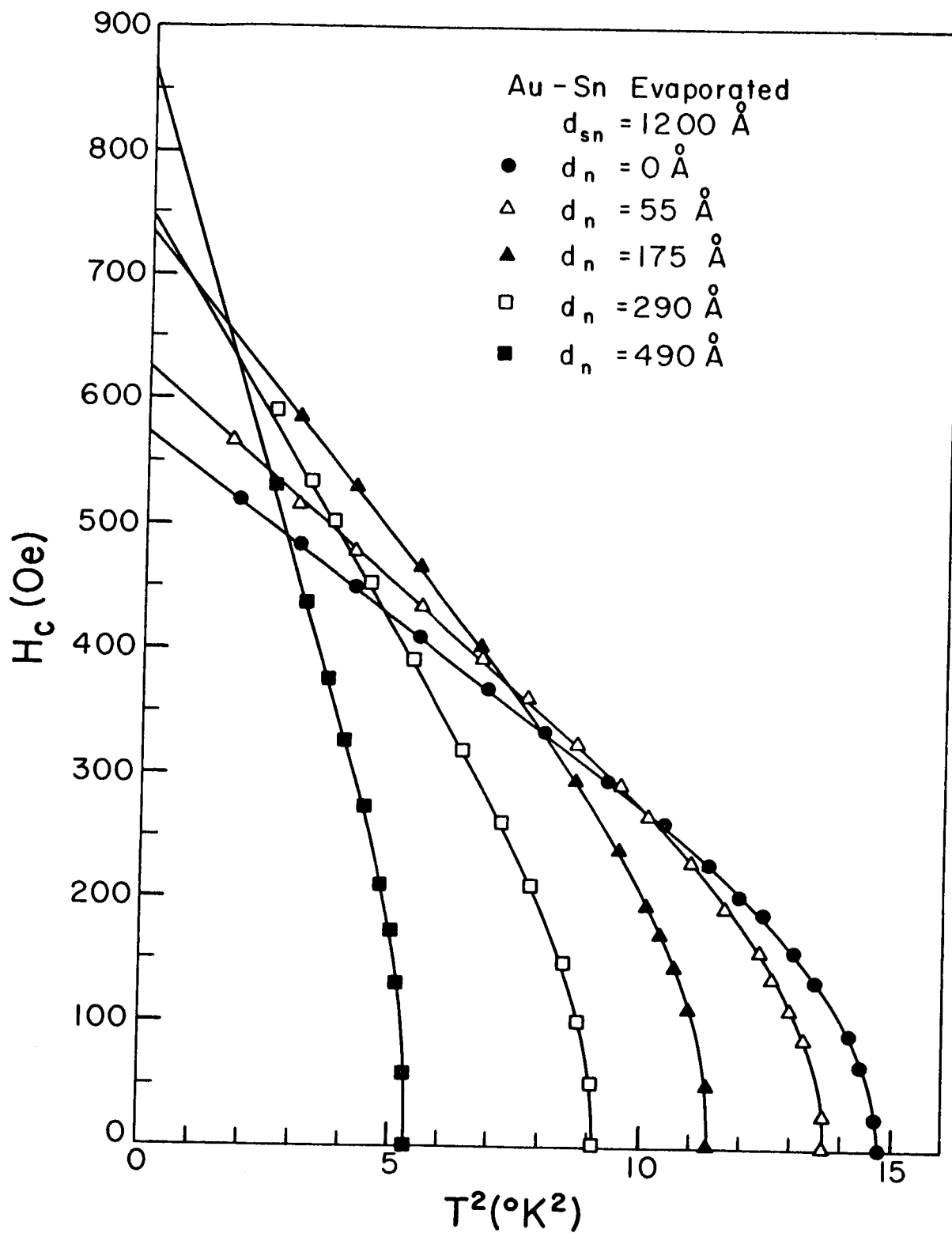


Fig 2
B-55986

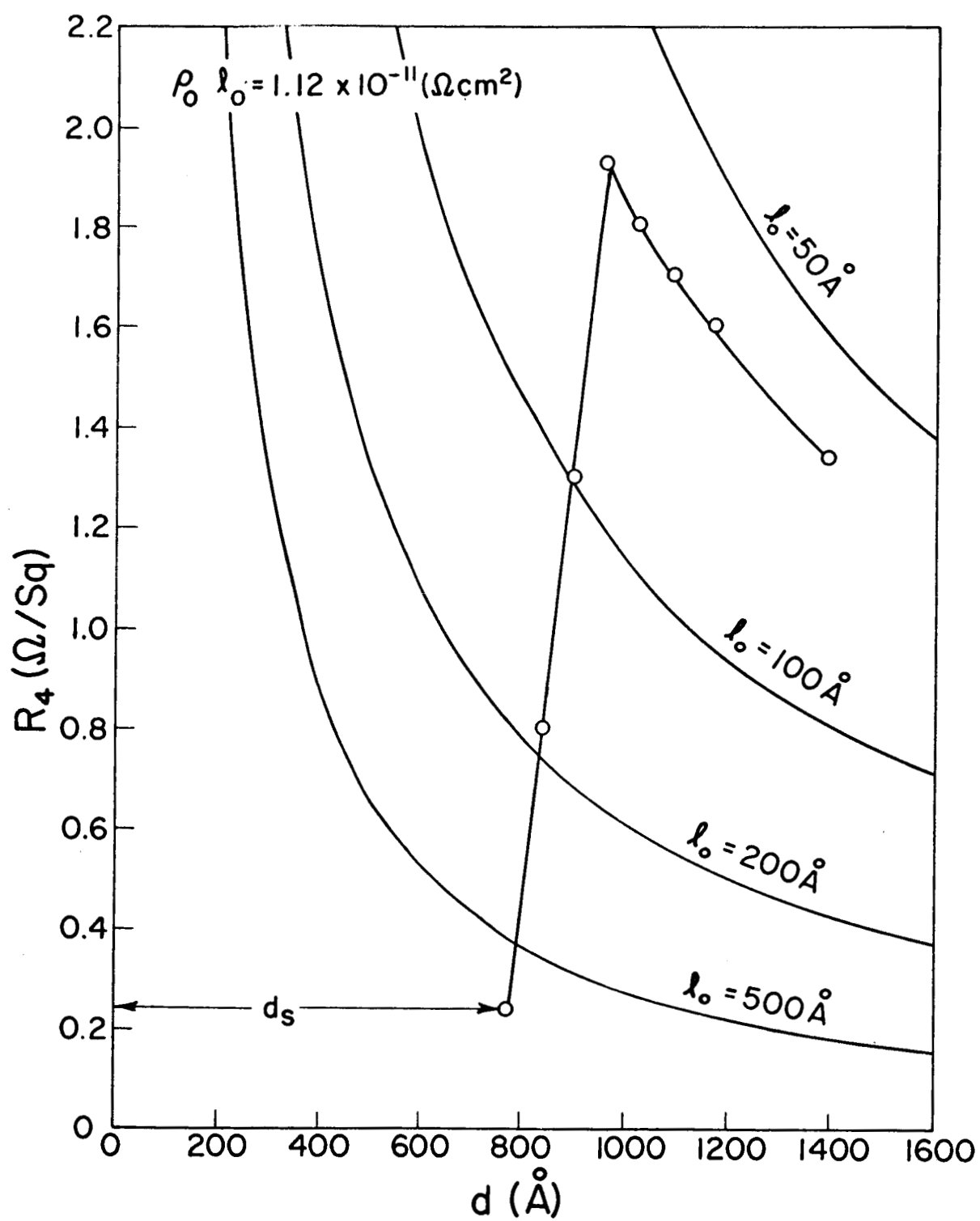


Fig. 3
8-55991

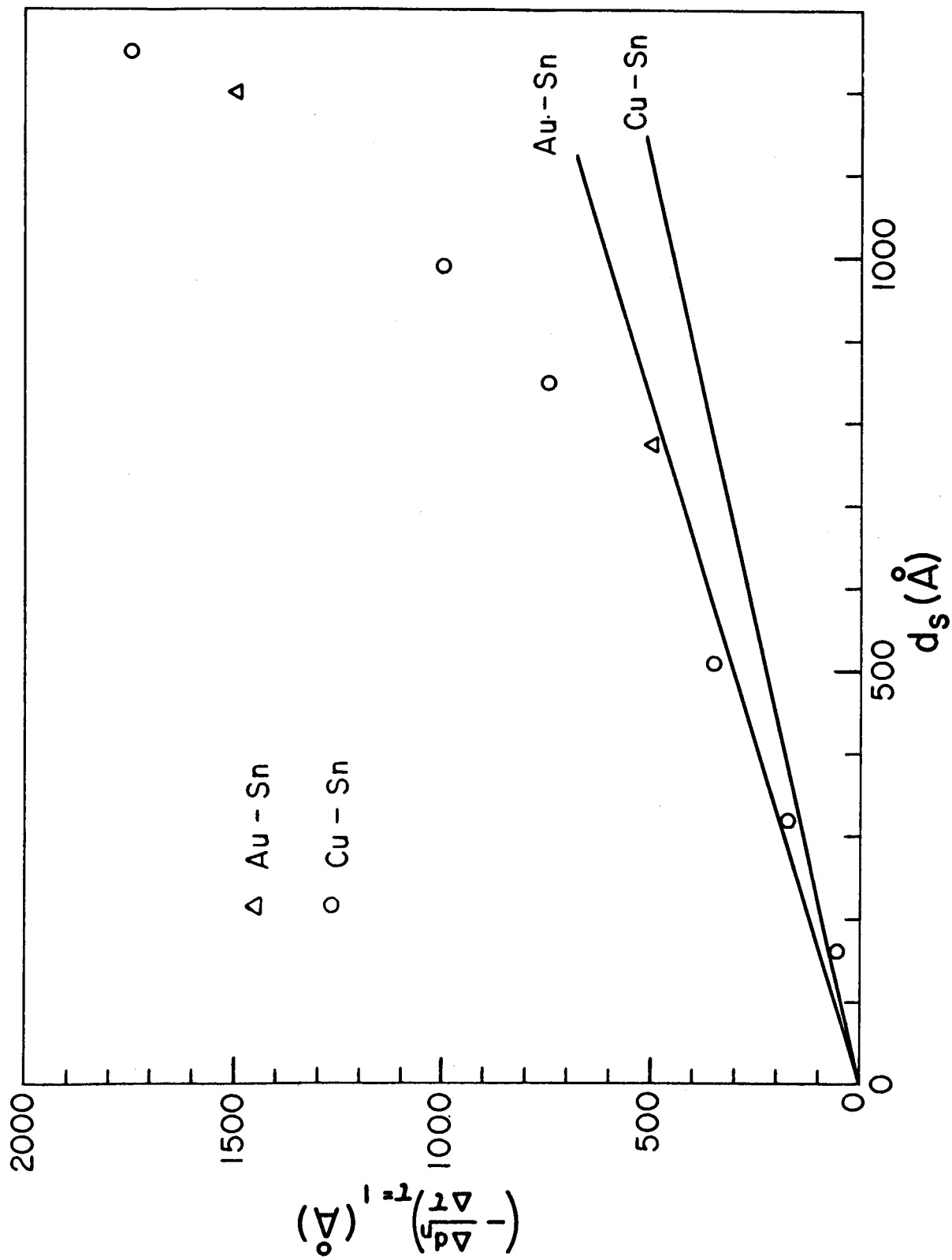


Fig. 4
B-55990

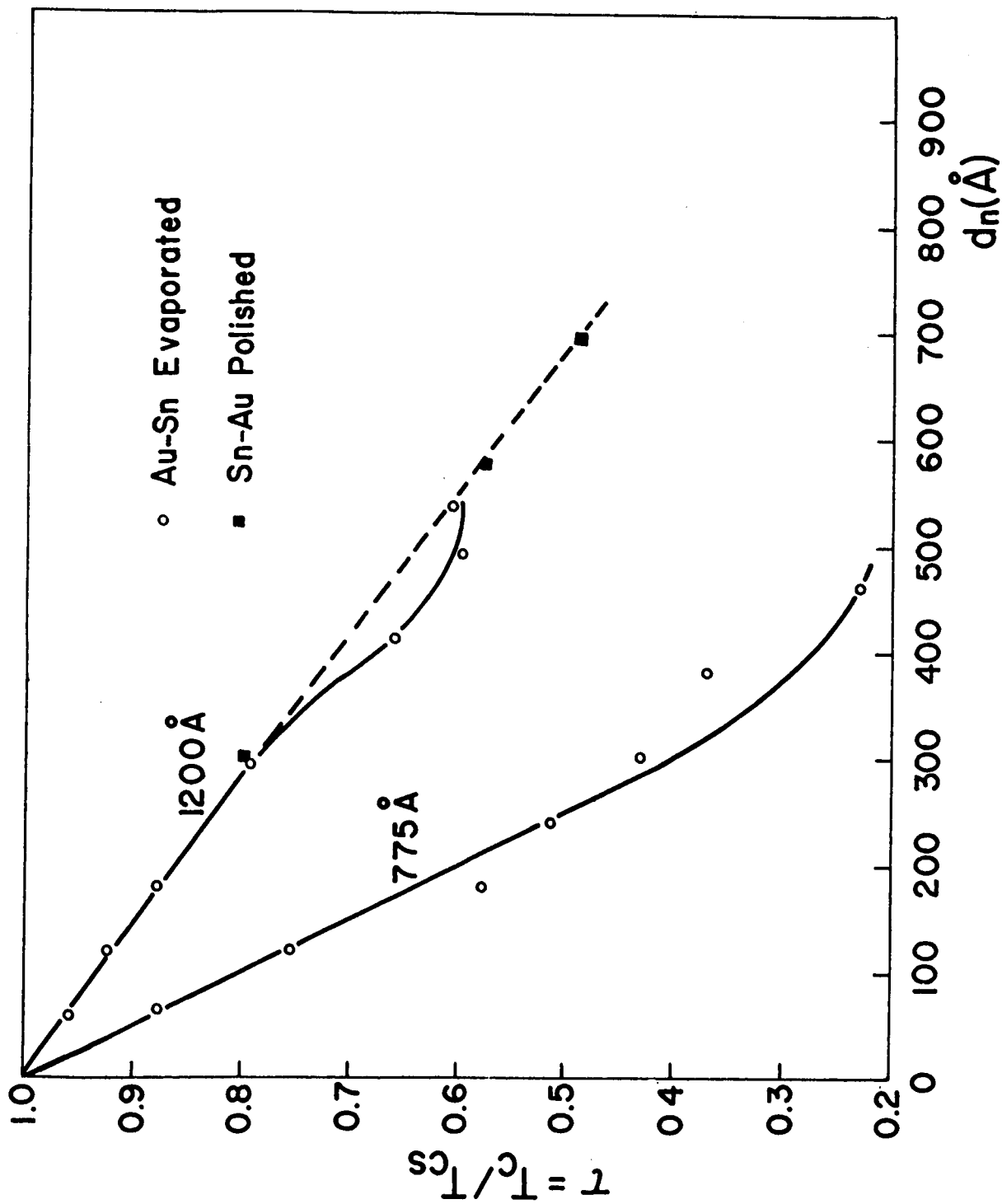


Fig. 5

B-55988

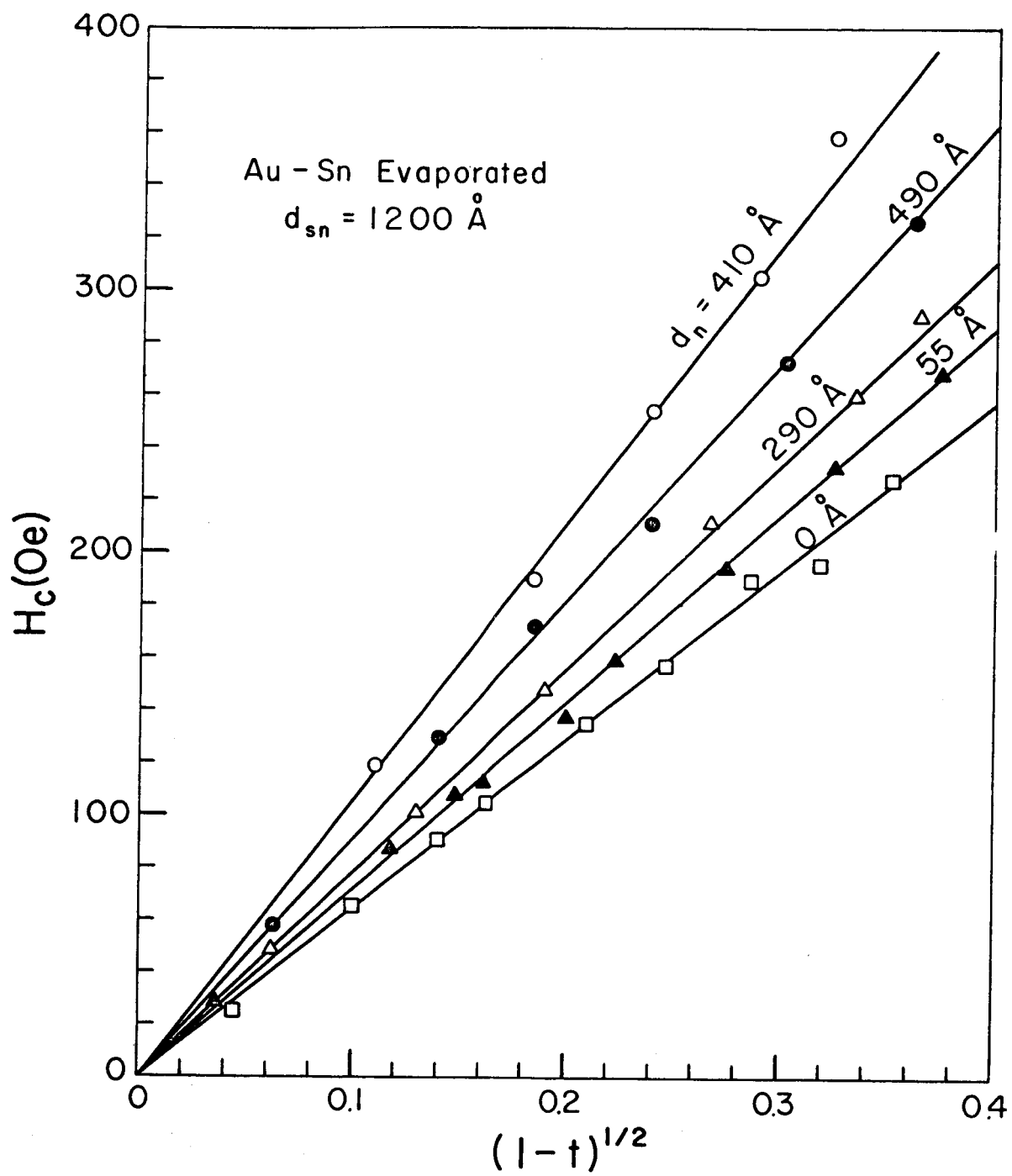
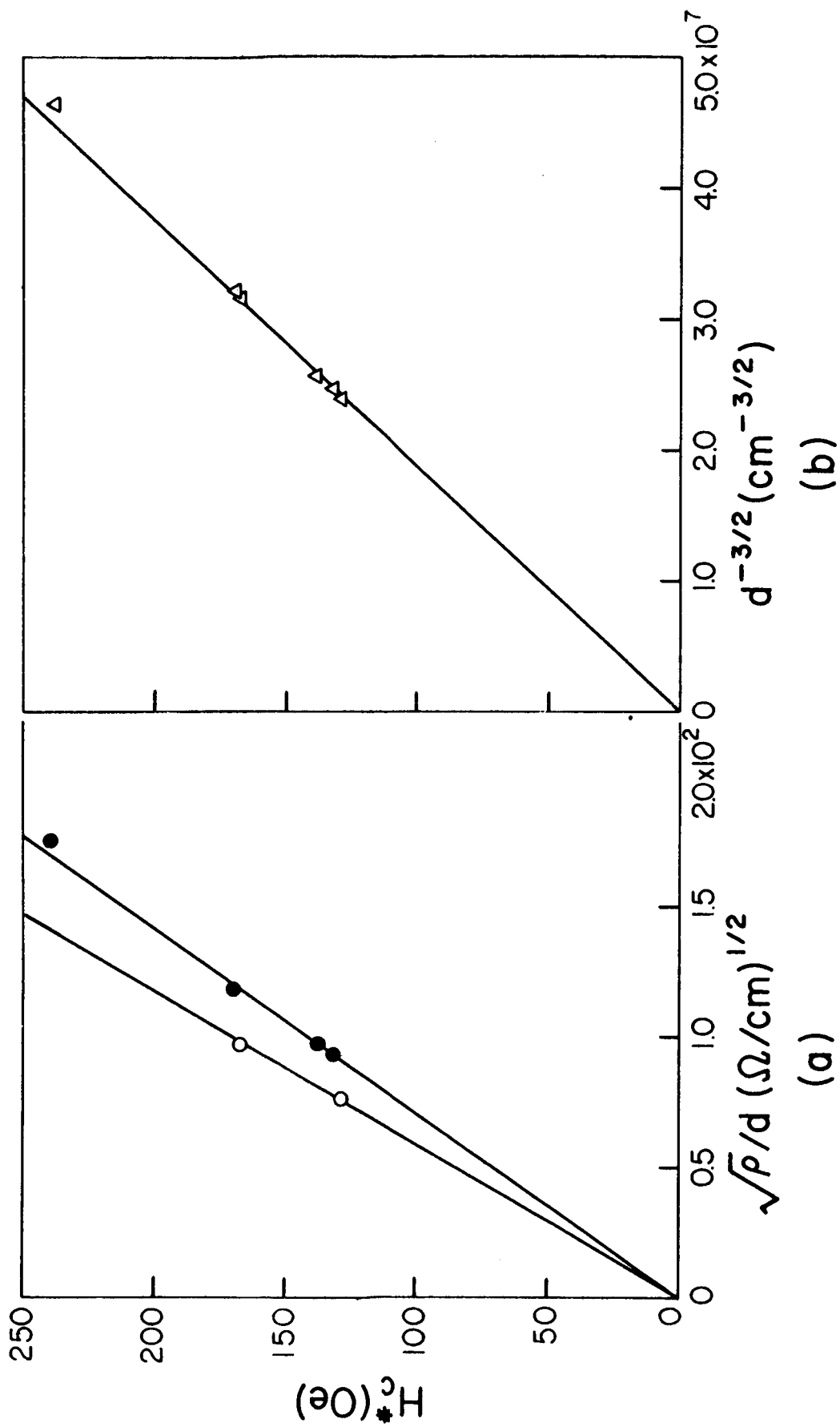


Fig 6
B-55987



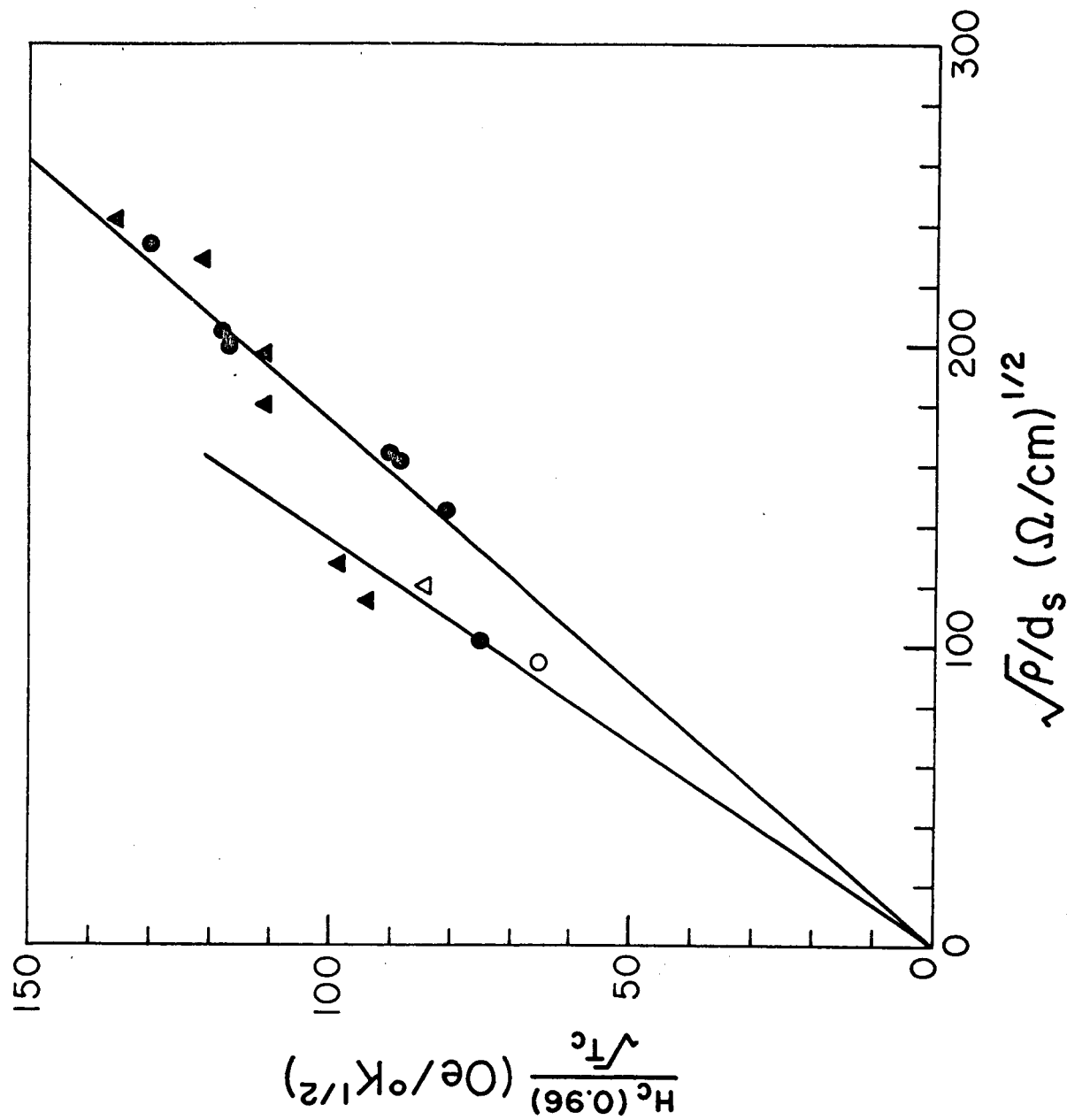


Fig. 8.

8-5593